Paper No.
13184

NACE INTERNATIONAL
CORROSION Conference & Expo 2019

Corrosion Inhibitor (Decanethiol) for Carbon Steels Exposed to Aqueous CO_2

Z. Belarbi, J.M. Dominguez Olivo, F. Farelas, M. Singer, D. Young, S. Nesic

Institute for Corrosion and Multiphase Technology,
Department of Chemical and Biomolecular Engineering,
Ohio University

Athens, OH 45701
USA

ABSTRACT

CO_2 corrosion mitigation is a challenge in the oil and gas industry. In order to decrease the severity of CO_2 corrosion of carbon steel pipelines and equipment, different mitigation practices are recommended. One such strategy is the application of surface active chemical inhibitors. The objective of this study was to evaluate the inhibition effectiveness of decanethiol in a CO_2-saturated aqueous electrolyte (1 wt.% NaCl). The inhibition properties of decanethiol were evaluated by electrochemical measurements (linear polarization resistance (LPR) and electrochemical impedance spectroscopy (EIS)) and the steel surface was characterized by scanning electron microscopy (SEM). The obtained data show that decanethiol can successfully prevent corrosion of carbon steels in a CO_2 environment. An inhibition mechanism was also proposed based on adsorption characteristics and inhibitor film formation.

Keywords: CO_2 corrosion, decanethiol, carbon steel, EIS, surface film.

INTRODUCTION

Carbon dioxide (CO_2) corrosion becomes a serious problem when, in the oil and gas industry, significant amounts of CO_2 dissolve in water causing corrosive degradation of facilities made from carbon steel. One way to minimize internal corrosion of carbon steel pipelines exposed to CO_2 environments is by injecting corrosion inhibitors. Most CO_2 corrosion inhibitors used in industry are organic compounds containing nitrogen, oxygen and/or sulfur. [1,2,3,4] The inhibitive action of these compounds is due to their adsorption at the metal surface. This process depends upon the nature and surface charge of the metal, the type of aggressive media present, the molecular structure of the inhibitor, and the nature of its interaction with the metal surface. In a previous study, Belarbi, *et al*.,[5] investigated the role of the potential of zero charge (PZC) and found that the corroding steel surface is positively charged with respect to the PZC in acidic environments; therefore, the adsorption of anions (e.g. ubiquitous Cl^-) or of inhibitor molecules with a negative structural moiety is favored.

The corrosion resistance of copper immersed in an aqueous solution containing dodecanethiol has been reported.[6] A dodecanethiol monolayer was determined to retard the reduction of dissolved oxygen and inhibited the growth of copper oxide in NaCl solution. In another study, weight loss measurements showed that similar alkanethiols are able to retard corrosion rates when steel specimens are exposed under top of the line corrosion (TLC) conditions.[7] Based on the results of these studies, thiols, especially decanethiol and 11-mercaptoundecanoic acid, showed superior mitigation of TLC.[7] Belarbi, *et* al.[8], investigated the effect of different operating parameters on the inhibition efficacy of decanethiol. The effect of water condensation rate, monoethylene glycol (MEG), hydrogen sulfide (H_2S) and hydrocarbon on inhibitor efficacy was evaluated. It was found that the presence of MEG, variation of gas temperatures and water condensation rates did not affect the inhibition efficacy of decanethiol. In sour environments, decanethiol was able to reduce localized corrosion of carbon steel exposed to 30 ppm H_2S. In the presence of a condensable hydrocarbon (heptane), decanethiol lost its inhibition efficacy and showed very poor persistency. However, in the absence of condensable hydrocarbons, decanethiol showed excellent persistency, filming behavior and superior mitigation of TLC.[7]

In a continuation of our research on understanding of inhibition mechanisms of CO_2 corrosion, the present work involves a systematic study of the inhibitive action of decanethiol on X65 carbon steel immersed in a NaCl solution saturated with CO_2. Despite a large number of corrosion inhibition investigations, minimal research has been reported on inhibition mechanisms involving thiols, particularly relating to the mitigation of carbon steel corrosion. Linear polarization resistance (LPR) and electrochemical impedance spectroscopy (EIS) analyses were carried out to understand the inhibition mechanism of carbon steel in the test electrolyte at ambient temperature. The adsorbed film was analyzed using X-ray photoelectron spectroscopy (XPS).

EXPERIMENTAL

Materials and Chemicals

Steel specimens used for electrochemical measurements were machined from an API [(1)] 5L X65 carbon steel with a tempered martensite microstructure. The chemical composition of this carbon steel is provided in Table 1. The electrolyte was prepared by dissolving sodium chloride (NaCl) in deionized water, which was then saturated with CO_2. Analytical grade decanethiol used in this study was acquired from Sigma-Aldrich†.

Table 1

Composition (wt.%) of the selected API[(1)] 5L X65 carbon steel

Element	C	Nb	Mn	P	S	Ti	V	Ni	Fe
Composition	0.05	0.03	1.51	0.004	<0.001	0.01	0.04	0.04	balance

Electrochemical Measurements

Investigation of the inhibiting properties of decanethiol on carbon steel corrosion was performed by electrochemical methods using LPR and EIS. The electrochemical measurements were carried out using a three-electrode glass cell configured as shown in Figure 1; key elements are a platinum grid as a counter electrode, $Ag/AgCl_{sat}$ electrode as a reference electrode, X65 carbon steel rotating cylinder electrode (RCE) as a working electrode, and an additional rectangular X65 carbon steel specimen (surface area = 1 cm^2) that was extracted for *ex situ* XPS analysis. All potentials reported in this paper are referred to an $Ag/AgCl_{sat}$ reference electrode. The reference electrode was placed in a separate chamber and was connected to the corrosion cell *via* a KCl salt bridge and a Luggin capillary. Prior to each experiment, the RCE was sequentially polished with silicon carbide paper (320, 400 and 600 grit), cleaned with isopropanol in an ultrasonic bath, and air-dried before introduction into the cell. The corrosion tests were performed in 1 wt.% NaCl at 25°C and 1 bar total pressure. The solution was deoxygenated for 2 hours by sparging with CO_2 prior to the introduction of the working electrode. The CO_2 saturated solution was maintained at pH 3.8 and was not affected by the injection of decanethiol. To avoid possible noise in electrochemical measurements caused by CO_2 sparging, the sparge tube was pulled up into the headspace during data acquisition. Purging with CO_2 was maintained throughout the test to prevent air ingress and maintain saturation of the test solution with CO_2. The rotation speed of the working RCE was set at 1000 rpm before starting the electrochemical measurements. Corrosion rate was assessed by LPR, by polarizing the working RCE from -5 mV to +5 mV measured from the OCP; using a scan rate of 0.125 mV/s and a B value of 26 mV. The B value for these experiments is taken from previous research conducted on mild steel in a CO_2 environment and was used in the analysis of all the experiments reported here.[5]

LPR and EIS data were taken every hour during a total exposure time of 6 hours. The electrochemical measurements were conducted with a Gamry‡ potentiostat/galvanostat. The full experimental matrix for electrochemical experiments is shown in Table 2. The concentrations of decanethiol were higher than the solubility limit (2.58 ppm_v at 25ºC). Therefore, a layer of the immiscible decanethiol formed at the top of the liquid phase. EIS data were acquired from 10 kHz to 0.1 Hz with 7 points per decade and an AC amplitude of 10 mV(rms). EIS scans were analyzed and fit using the software SIMAD§ (*Laboratory Interfaces et Systèmes Electrochimiques–France*), which allowed fitting both the frequency-dependent analytical expressions and equivalent electrical circuits.

Cathodic Potentiodynamic polarization sweeps were measured at the final of the experiment when the corrosion rates were stable, by starting from the open circuit potential up to -1.2 V at a scan rate of 0.125 mV/s. The anodic potentiodynamic sweeps were taken when the OCP was stable again. The sweeps were taken from the OCP up to +400 mV. The ohmic drop was accounted for in all the curves.

(1) American Petroleum Institute (API), 1220 L St. NW, Washington, DC 20005.

‡ Trade name
§ Trade name

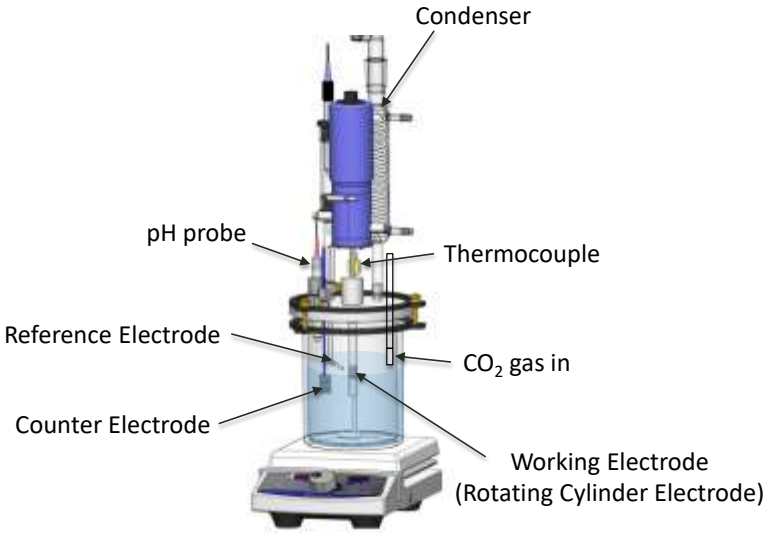

Figure 1: Experimental setup for electrochemical tests

Table 2
Experimental matrix for electrochemical tests

Total pressure (bar)	1
pCO_2 (bar)	0.96
Solution	1 wt.% NaCl
Solution temperature	25°C
Working electrode	X65 carbon steel
Decanethiol concentration (ppm_v)	0, 5, 10, 100, 400
RCE rotation speed (rpm)	1000

Surface Analysis

At the end of each experiment, the steel surface was characterized by a scanning electron microscopy (SEM; JEOL JSM-6090 LV*) . Imaging was performed at an accelerating voltage of 15 kV using a secondary electron signal (SE). The X-ray photoelectron spectroscopy (XPS) was performed in a VG Scientific ESCALAB**MKII spectrometer using Al Kα (1486.6 eV) radiation. The instrumental resolution was 1.2 eV with a slit width of 0.6 cm. Samples were maintained at ambient temperature at a pressure of 5×10^{-9} mbar.

RESULTS AND DISCUSSION

LPR Corrosion Rate

Each experiment was started with a freshly polished electrode. The electrode was first left at the OCP conditions for 1 hour. Then, the LPR was recorded. The evolution of the corrosion rates (CR) and the open circuit potential (OCP) measurements with time for the X65 carbon steel specimens, exposed to a

* Trade name
** Trade name

1 wt.% NaCl solution saturated with CO_2 at 25ºC in the absence and in the presence of various concentrations of decanethiol, are displayed in Figure 2. In the absence of decanethiol, the corrosion rate (CR) was approximately 3 mmy^{-1} and the OCP was -0.68 V vs. $Ag/AgCl_{sat}$. In the presence of decanethiol, the final corrosion rate decreased to reach a low value of 0.02 mmy^{-1}, while the OCP shifted to more anodic values. Such an effect could be due to the retardation in both the anodic and cathodic reactions at the steel surface (caused by adsorption of the inhibitor). Figure 3 shows the potentiodynamic polarization curves for the CO_2 corrosion of steel at different thiol concentrations. It can be observed that both cathodic and anodic reactions were retarded by the presence of thiols. At a first glance, the addition of 5 ppm_v of thiols seemed to retard the anodic reaction more than the cathodic. However, as explained by Dominguez, *et al.*[9,10], this effect is due to the adsorption of organic corrosion inhibitors: only charge transfer reactions are retarded while limiting currents remain unaffected. This condition produces an increase in the OCP. Such an effect is also seen with the addition of 10 ppm_v of thiol, as the charge transfer reactions were more retarded while the limiting current remained unaffected. After the addition of 100 ppm_v, the hydrogen evolution reaction was more altered. This could be explained by the formation of a self-assembled monolayer (SAM) in the metal surface due to the immersion of the iron specimen into a high concentrated/saturated solution of decanethiol, which is due to the immiscible layer of decanethiol formed at the top of the liquid phase. Such an immersion could potentially develop a SAM (such as a Langmuir-Blodgett film[11]). Langmuir-Blodgett films have been reported to significantly modify the nature of the charge transfer process, including the electrochemical reactions associated with corrosion of iron.[11,12]. The LPR results were complemented with EIS measurements.

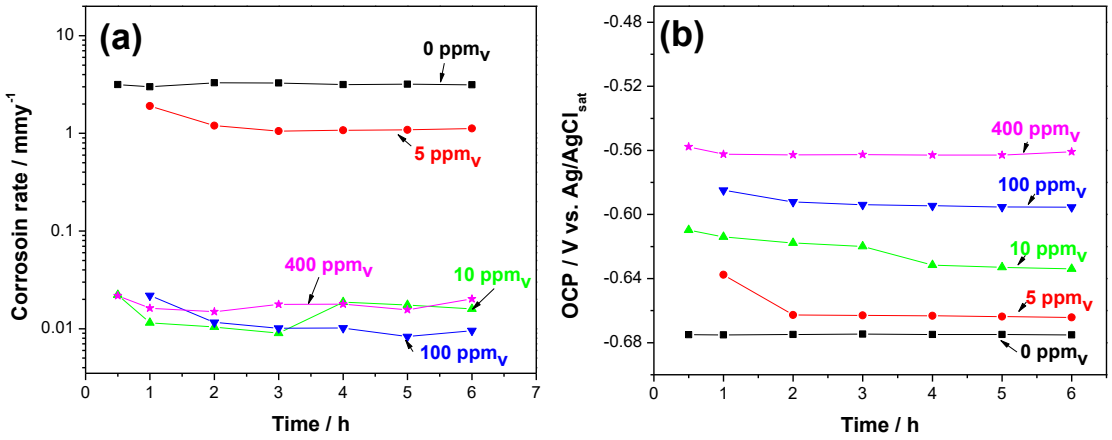

Figure 2: Corrosion rate (a) and open circuit potential (b) of the X65 carbon steel immersed in 1 wt.% NaCl solution in the presence and absence of inhibitor at 25ºC as a function of time

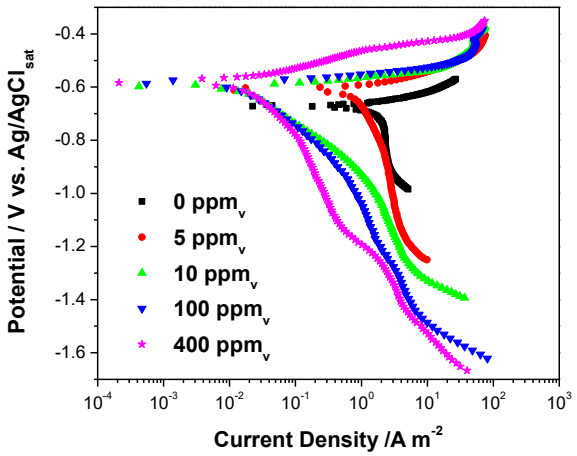

Figure 3: Potentiodynamic polarization curve of CO_2 at different concentrations of decanethiol

EIS

The LPR results were complemented with EIS measurements. Results obtained in a 1 wt.% NaCl solution, after 6h of immersion at the corrosion potential E_{corr} without and with decanethiol are presented in Figure 4 and Figure 5, respectively. The corrosion behavior of carbon steel in CO_2 environments is well researched. [4,5,7,13] In the absence of inhibitor and at the E_{corr}, the Nyquist diagram (Figure 4a and Figure 4b) exhibit single depressed semicircles at high to medium frequencies. Belarbi, *et al.*[4], have reported an inductive loop at low frequency (LF) range (< 0.1 Hz) which may be attributed to the relaxation process obtained by adsorbed species such as Cl^-_{ads} and H^+_{ads} on the electrode surface. Epelboin and Keddam[14] showed that the inductive loop observed at low frequency could be attributed to partial coverage of the iron surface by an adsorbed intermediate. As usually indicated in an EIS study, the high frequency (HF) capacitive loop is related to the charge-transfer resistance (R_t) process of the metal corrosion and the double-layer behavior. These loops are not perfect semicircles; such behavior is characteristic for non-uniform metal surfaces (*i.e.*, increased surface roughness).[15] In an analysis of such cases, the double layer capacitance, $C_{dl,}$ is replaced by a so-called “constant phase element” (CPE).

In the presence of decanethiol, the low-frequency limit of the impedance loop increased (Figure 4a and Figure 4b), indicating increased polarization resistance. In addition, the impedance modulus value in the uninhibited solution was much smaller than that in the inhibited solution (Figure 5a) and reached a maximum at a concentration of 100 ppm_v. In addition to the time constant of the charge transfer process and the double layer capacitance, a second-time constant was observed in the high-frequency domain after adding decanethiol at concentrations higher than 10 ppm_v (Figure 5b). This second time constant could be attributed to the adsorbed inhibitor film on the steel surface.[4]

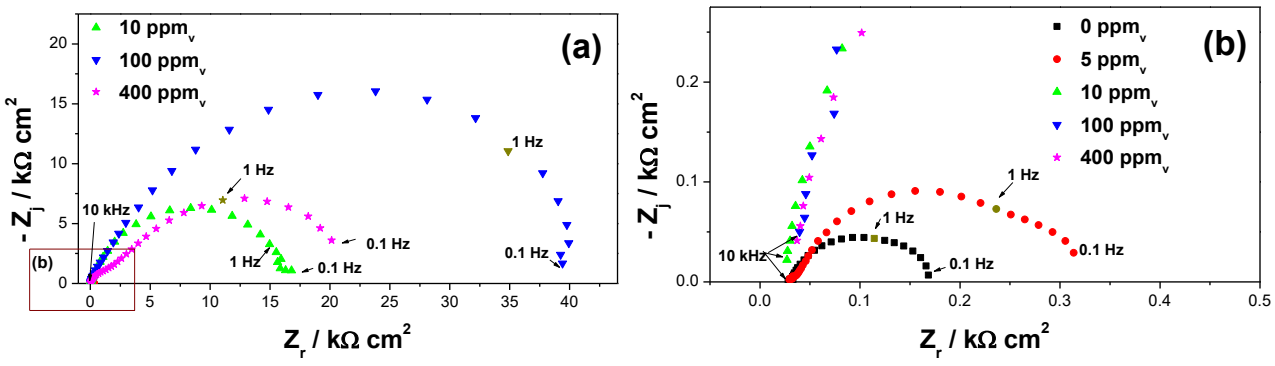

Figure 4: Nyquist diagrams of carbon steel immersed in CO_2-saturated 1 wt.% NaCl solution after 6 h in the presence and absence of decanethiol at 25°C (a), Zoom in at the Nyquist plot at high frequencies(b)

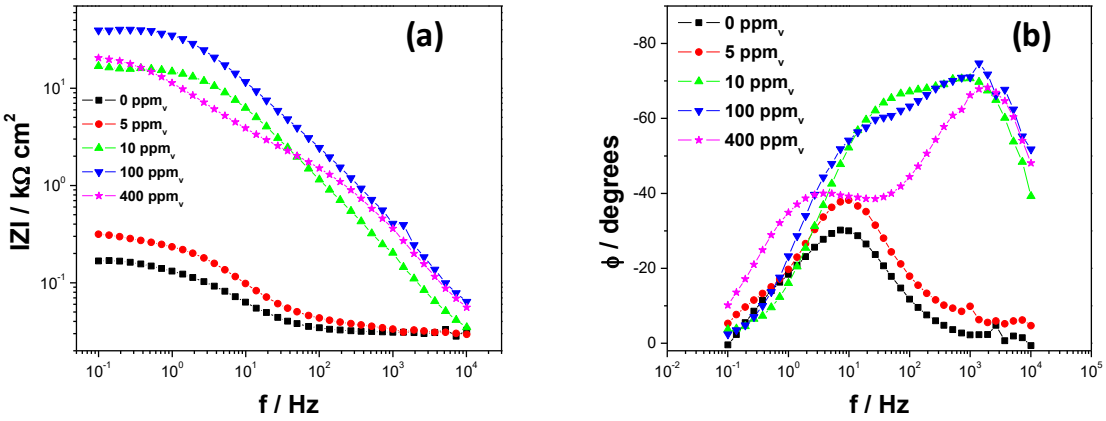

Figure 5: Bode diagrams of carbon steel immersed in 1 wt.% NaCl solution after 6h in the presence and absence of decanethiol at 25°C: (a) modulus; (b) phase

The thickness of the inhibitor layer can be estimated from the EIS measurements through calculation of the double layer capacitance C_{dl} and the inhibitor film capacitance C_f values. In the absence of inhibitor, the impedance spectra (Figure 6a) were fitted to the electrical equivalent circuit presented in Figure 6b. Most typical EIS diagrams conducted at ambient temperature and in NaCl solutions saturated with CO_2 at atmospheric pressure contain a high frequency (HF) capacitive loop followed by an inductive loop at low frequency (LF).[5,13,16-19] Almeida *et al*.[18] showed that the capacitive loop associated with the charge transfer resistance in parallel with the double layer capacitance. An additional contribution, either inductive or capacitive can also be observed at lower frequencies, in the mHz domain. The inductive loop was explained by the relaxation of $(FeOH)_{ads}$ and $(FeCO_2)_{ads}$ adsorbed on the iron surface. Almeida *et al.*[18] developed a better analysis of CO_2 corrosion by calculating the impedance diagrams considering the Langmuir-type adsorption isotherm, in which the fractions of the electrode surface filled by intermediate species $Fe(I)_{ads}$, $(FeOH)_{ads}$ and $(FeCO_2)_{ads}$. The analytical expression of impedance calculated by Almeida *et al.*,[18], can be represented by the electric circuit in figure 5b. These circuits consist of R_s (the resistance of solution between the working electrode and counter electrode), C_{dl} in parallel to the R_t (charge-transfer resistance), and R_t in parallel with the inductive elements L (inductance) and R_L (inductive resistance).

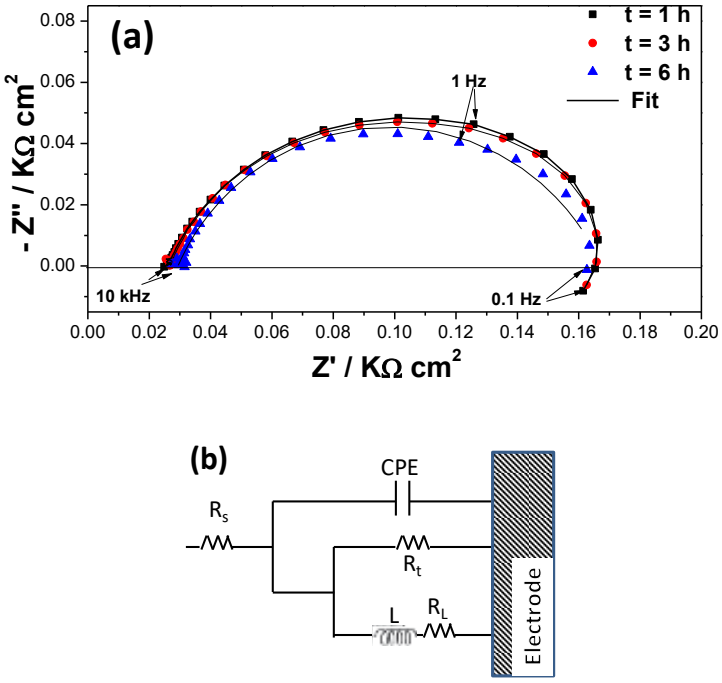

Figure 6: Experimental and fitted data of carbon steel immersed in 1 wt.% NaCl solution in the absence of inhibitor at 25°C (a) and (b) equivalent circuit used for the regression calculation

In the presence of 100 ppm_v of decanethiol (Figure 7a), the low-frequency response and its evolution with immersion time are different from the uninhibited solution. The inductive loop in the low-frequency range disappears. The same behavior was observed at 5, 10 and 400 ppm_v of decanethiol (the impedance diagrams are not presented in this manuscript). This could be due to the shift of the inductive loop at low frequencies that we could not see in the range of the studied frequencies. In addition to the time constant of the charge transfer process and the double layer capacitance, a second-time constant was observed in the high-frequency domain after adding decanethiol at concentrations higher than 10 ppm_v. LPR and potentiodynamic sweeps results suggested that the decanethiol retards the charge transfer reactions and forms a self-assembled monolayer on the steel surface. Therefore, the impedance diagrams obtained at each time and for different concentrations (5, 10, 100 and 400 ppm_v) were fitted to the electrical equivalent circuit presented in Figure 7b. The time constant in the high-frequency range (order of kHz), $R_f C_f$, is attributed to inhibitor film adsorption. C_f and R_f are the capacitance and the resistance associated with the inhibitor film, respectively. The time constant at low frequencies (~ 10 Hz), $R_t C_{dl}$ is related to the electrochemical reactions at steel surface.

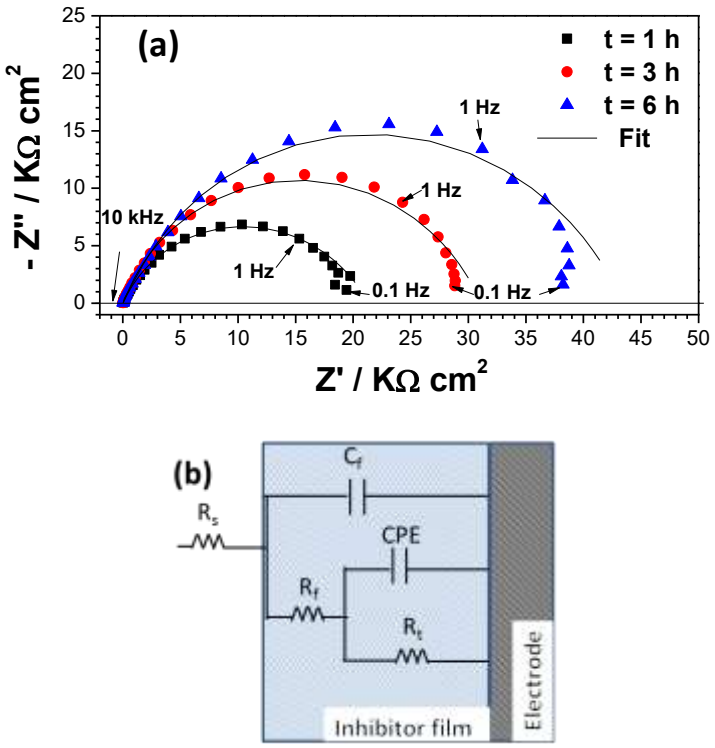

Figure 7: Experimental and fitted data of carbon steel immersed in 1% wt. NaCl solution in presence of 100 ppm_v of decanethiol at 25°C (a) and (b) equivalent circuit used for the regression calculation

The good agreement between the experimental and fitted data enabled the determination of R_s, Q_{dl}, α, R_t, C_f, and R_f. Brug, et *al.*,[20] developed a theory, assuming uniform resistances on the electrode surface and a distributed capacitance, leading to the following equation to calculate the value of C_{dl} as a function of R_s, double layer CPE coefficient Q_{dl} and α:

$$C_{dl} = R_s^{\frac{(1-\alpha)}{\alpha}} Q_{dl}^{\frac{1}{\alpha}} \quad (1)$$

Variations of C_{dl}, R_t, C_f, and R_f with immersion time are presented in Figure 8. The solution resistance R_s is around 6±1 Ω. In the absence of decanethiol, the R_t magnitude associated with the charge transfer shows a slight change with time ranging from 158 Ω to 142 Ω. In the literature[13,21, 22,23], it has been postulated that the decrease of R_t was a consequence of the continuous dissolution of the ferrite phase and due to the increase of the cementite (Fe_3C) covered surface area which enhances the galvanic effect associated with Fe_3C. However, the increase of decanethiol concentration generally led to an increase of R_t and decrease of C_{dl}. This could be due to the inhibitor adsorption across the steel surface that retards the charge transfer reactions, thus lowering the corrosion rate. The EIS results were in good agreement with the potentiodynamic polarization curves. In addition, the increase of decanethiol concentration above 10 ppm_v leads to the formation of a self-assembled monolayer (SAM) that will lead to a decrease in C_{dl}. Based on these results, it can be inferred that the threshold concentration for decanethiol in 1% wt. NaCl solution is between 10 and 100 ppm_v. However, increasing the concentration of decanethiol above 100 ppm_v, will not improve the inhibition efficacy. The film thickness is much thicker when different decanethiol concentrations are added to the solution.

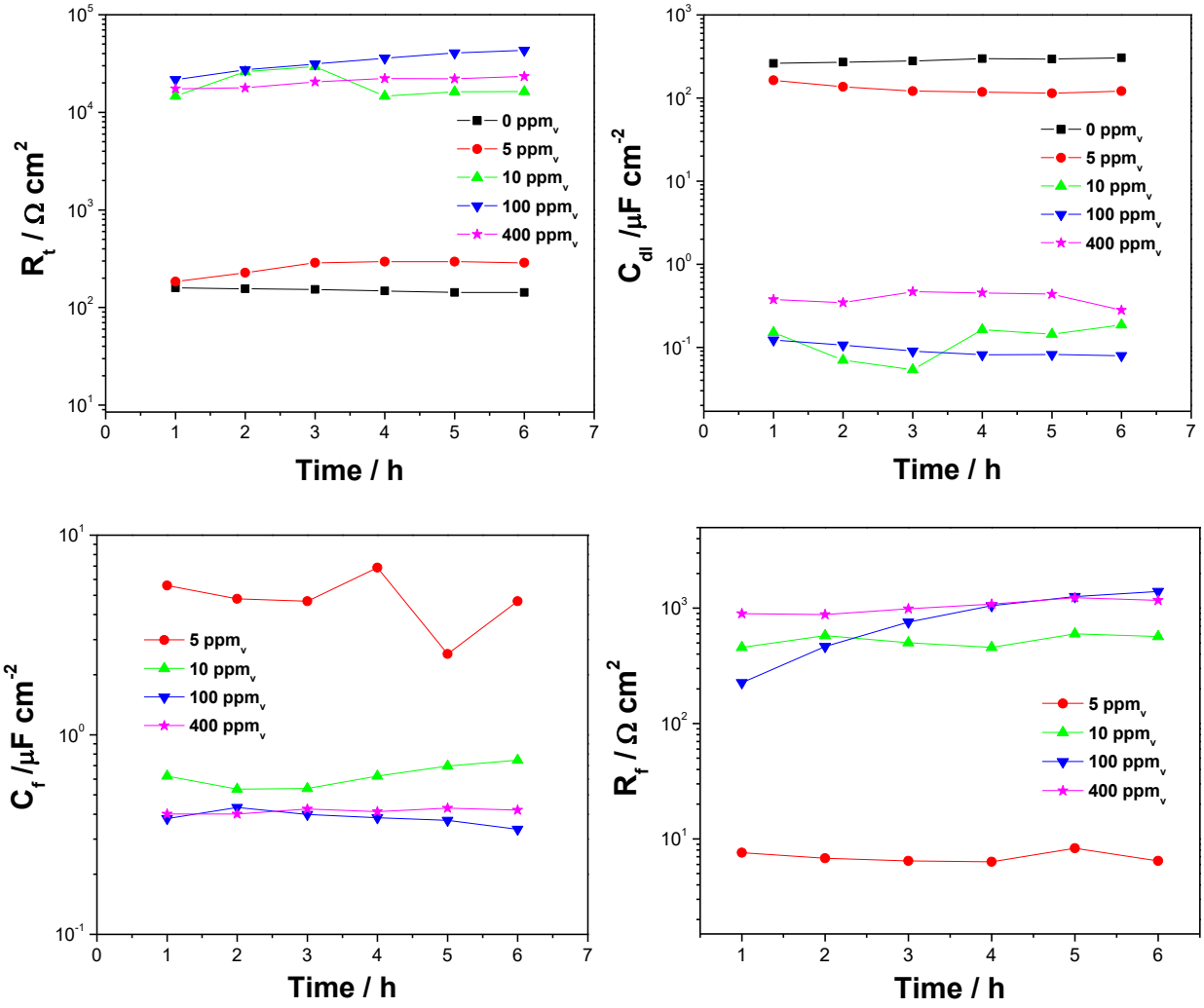

Figure 8: Variation of R_t, C_{dl}, C_f *and* R_f. *vs*. time

If the planar condenser model (parallel plate model) is assumed[24], then one can relate the capacitance C_f and the film thickness d by Equation (2):[24]

$$C_f = \frac{\varepsilon\varepsilon_0}{d} \quad (2)$$

where ε_0 is the permittivity of the vacuum (9 x 10^{-14} F cm^{-1}), ε is the dielectric constant of inhibitor and d is the thickness of the inhibitor film. The average value of the dielectric constant for alkanethiolate is around 2.1.[25,26] If we assume that $\varepsilon = 2.1$, the average calculated thickness "*d*" of the inhibitor layer from Equation (2) using the C_f (Figure 8) would be 0.4 nm, 3 nm, 5 nm and 5 nm at 5, 10, 100 and 400 ppm_v, respectively, after exposing carbon steel for 6h to an inhibited solution (Figure 9). Based on the tail length, obtained for decanethiol and the thickness determined by EIS, the thickness of 3 and 5 nm at 10 ppm_v and 100 ppm_v, approximately corresponds to one and two decanethiol molecular lengths, respectively. However, the thickness obtained at 5 ppm_v is lower than a one decanethiol molecular length, which could be due to the tilt angle between the surface and the decanethiol molecule. Based on the result reported in the literature, the formation of a first adsorbed layer could be due to electrostatic interactions between the inhibitor and the metal surface.[7] The second layer [12,27] would be formed with a further increase in inhibitor concentration with hydrocarbon tails interacting with each other and the hydrophilic group pointing toward the solution.

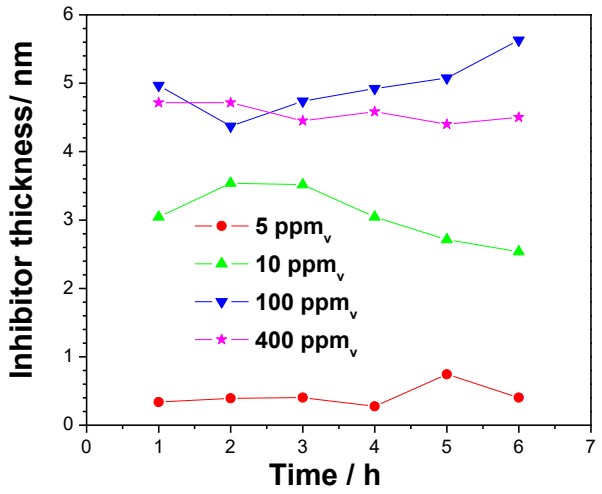

Figure 9: Variation of inhibitor thickness vs**.** time

Surface Characterization

SEM analysis

Figure 10 shows the SEM images of surface morphological features on the carbon steel specimens after electrochemical measurements. It is evident that, without inhibitor, corrosion products formed on the carbon steel surface. In the presence of 5 ppm$_v$ decanethiol, the steel surface was only partially protected. The SEM images show alternating corroded and protected areas. However, in the presence of decanethiol at 10, 100 and 400 ppmv, no corrosion was apparent and the scratch marks resulting from specimen polishing remained clearly visible after 6h of exposure to the 1 wt.% NaCl electrolyte. The surface of the carbon steel was well protected. These observations are in good agreement with the electrochemical results.

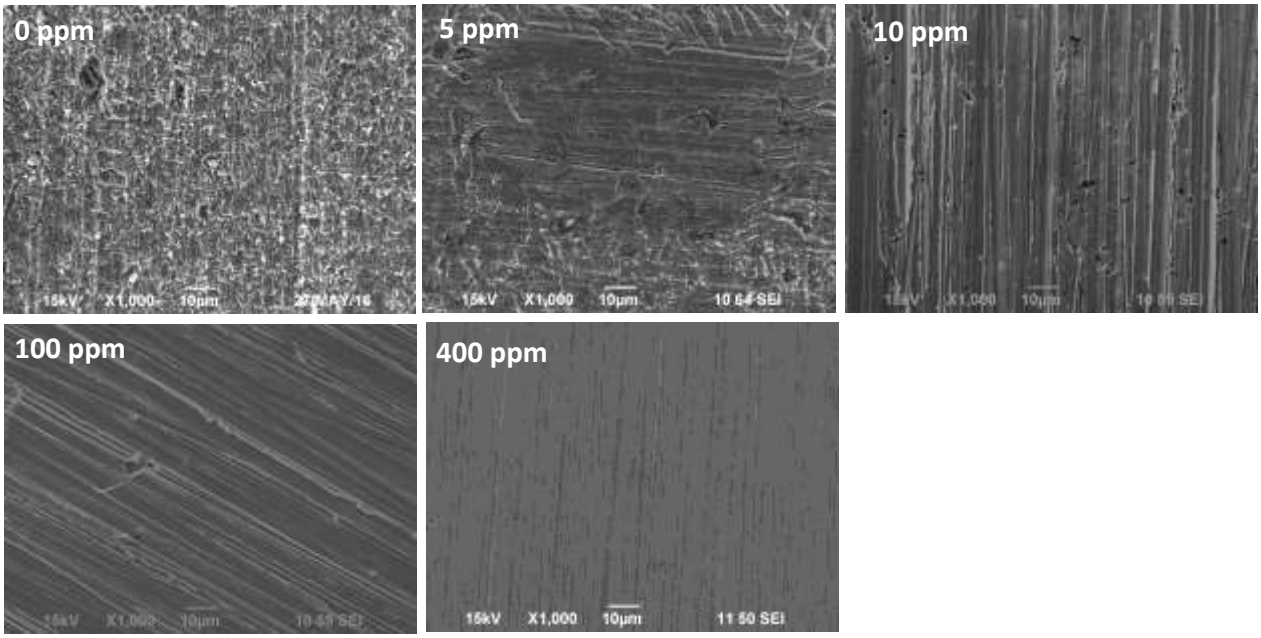

Figure 10: Surface morphology of carbon steels after 6 hours of immersion in a 1 wt.% NaCl electrolyte after 6 h in the presence and absence of decanethiol

Investigation of the interaction between thiol and the steel surface using X-ray photoelectron spectroscopy (XPS)

Inhibitor films adsorbed on the steel surface, after 6 hours of immersion in a 1 wt.% NaCl electrolyte in the presence of 400 ppm decanethiol, were characterized by ex-situ XPS analysis. XPS analysis was used to determine which elements were present on the electrode surfaces before and after exposure to the inhibitor solution. High-resolution scans of the Fe2p, O1s, C1s and S2p peaks were acquired from one spot on each sample using pass energy of 1486.6 eV to examine the type of chemical species present.

The results are presented in Figure 11. The recorded spectra for the "blank" reference sample (a freshly polished carbon steel) and carbon steel treated with decanethiol show a set of peaks characteristic of metallic (Fe) and oxidized iron. Two binding energies of 707.1 eV for Fe $2p_{3/2}$ and 720.2 eV for Fe $2p_{1/2}$ were observed, corresponding to Fe 2p of metallic iron. [28] The peaks around 710 eV for Fe $2p_{3/2}$ and 724 eV for Fe $2p_{1/2}$ correspond to the Fe 2p signatures of oxidized iron species.[28] The characterization of the inhibitor films adsorbed on the steel surface was completed by the analysis of the O 1s, C 1s, and S 2p spectral regions. The O 1s binding energy spectrum of the bare electrode showed evidence for the presence of oxidized iron species (530.4 eV). In the presence of decanethiol, the overall O 1s spectrum was deconvoluted into two peaks with binding energies of 530.4 eV and 532 eV, reflecting the presence of oxidized iron species and oxidized sulfur (S-O) on the steel surface, respectively. The element S is present as soon as the sample was immersed in NaCl with decanethiol. The energy levels of S 2p at 164 eV and 169 eV are compatible with the presence of the free thiol and oxidized sulfur (sulfate or sulfite), respectively. There is no binding energy peak belonging to Fe-S at 162.1 eV, meaning there is no chemisorption of decanethiol on the steel surface.[29] The binding energy peak belonging to oxidized sulfur can be postulated to mean that decanethiol adsorbed on the steel surface is unstable in air. For the bare steel surface, there is no comparable binding energy peak assignable to sulfur in this range. The C 1s XPS spectra were fitted by two peaks at 286 eV and 289-290.5 eV. The peak observed at 286 eV is assigned to carbon atoms of C–C bonds. This peak, which is due to contamination, is common in XPS and used as an energy reference. It is usually ascribed to oils residues associated with the vacuum system of the spectrometer. The intensity of the peak at 286 eV increased in the presence of inhibitor; therefore, the presence of C-C bonding could also be related to the inhibitor alkyl tail. All these results support the physisorption of decanethiol on the steel surface. Belarbi, *et al*.,[7] discussed the possible interactions between the steel surface and thiols. It has been reported that the sulfur atom (heteroatom) possesses a free electron pair which can establish Van der Waals secondary bonding interactions with the steel surface.

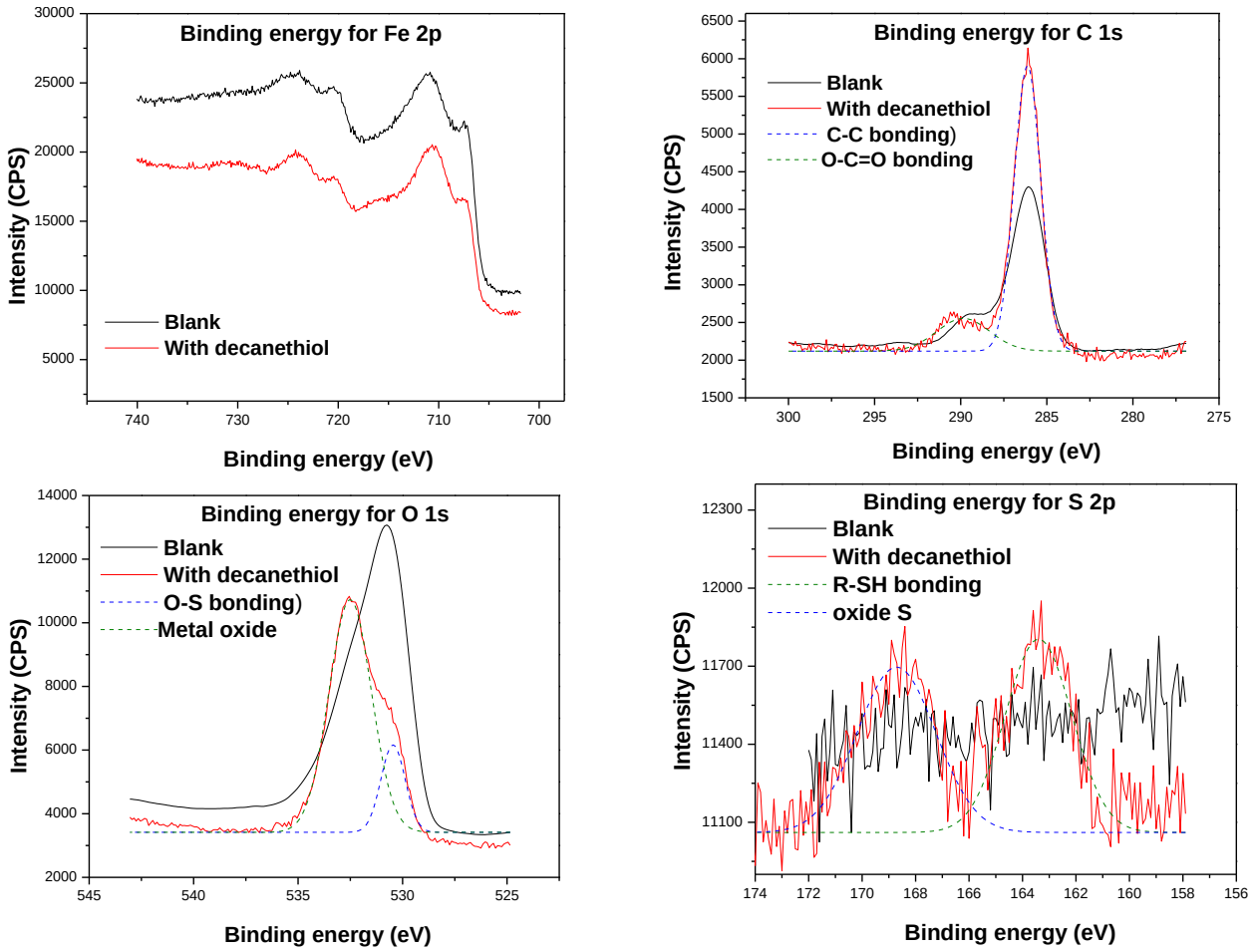

Figure 11: XPS spectra of bare steel (blank) and steel electrode immersed in NaCl solution after 6 hours in the presence of 400 ppm_v of decanethiol

CONCLUSIONS

In this study, the CO_2 corrosion resistance of carbon steel immersed in an uninhibited and inhibited NaCl solutions was studied by electrochemical measurements (EIS and LPR) followed by SEM characterization of corrosion products. The inhibition mechanisms were further investigated by studying inhibitor interactions at the steel surface using XPS. The key points of the present study are summarized as follows:

- *In situ* EIS confirmed the formation of an inhibitor film on the carbon steel surface immersed in the CO_2-saturated aqueous solution, resulting in a decrease in corrosion rates as determined by electrochemical measurements.
- The low-frequency impedance response of carbon steel at the corrosion potential and its evolution with time of immersion are different with and without inhibitor, showing that the inhibitor clearly influenced the electrochemical process at the steel surface. This analysis shows that the presence of inhibitor decreased the capacitance of the double layer.
- The film thickness was determined for decanethiol using electrochemical impedance spectroscopy and corresponded to a mono- or bi-layer structure.

- XPS analysis suggests physisorption of decanethiol on the steel surface as no primary chemical bond formed between metal and sulfur (Fe-S bond) could be identified.

ACKNOWLEDGMENTS

The authors would like to thank the following companies for their financial support: Quadrant Energy, BHP Billiton, BP, Chevron, ConocoPhillips, MI-Swaco, Petronas, PTTEP, Woodside, and Repsol. The authors are grateful to Prof. David Ingram of the "Edwards Accelerator Laboratory—Ohio University" for his help on *ex-situ* XPS experiments. Also, the technical support from the lab's staff at the Institute for Corrosion and Multiphase Technology by Mr. Alexis Barxias and Mr. Cody Shafer is highly appreciated. The authors are grateful to the "Laboratoire Interfaces et Systèmes Electrochimiques – Pierre and Marie Curie University, France" for the software SIMAD.

REFERENCES

1. R.L. Martin, "Inhibition of Vapor Phase Corrosion in Gas Pipelines," in CORROSION/97, paper no. 337, Houston, TX: NACE 1997.

2. R.L. Martin, "Inhibition of hydrogen permeation in steels corroding in sour fluids," Corrosion, vol. 49, no. 8, pp. 694-701, 1993.

3. R.L. Martin, "Control of top-of-line corrosion in a sour gas gathering pipeline with corrosion inhibitors," in CORROSION/2009, paper no. 09288, Houston, TX: NACE 2009.

4. Z. Belarbi, B. Brown, M. Singer and S. Nesic, " Study of Adsorption of Corrosion Inhibitor 1-(2-aminoethyl)-2-oleyl-2-imidazolinium Chloride on Carbon Steel Under CO_2 Environment by Using In-Situ AFM Measurements," in CORROSION/2017, paper no. 0990, Houston, TX: NACE 2017.

5. Z. Belarbi, F. Farelas, M. Singer and S. Nesic, "Role of amines in the mitigation of CO_2 Top of the Line Corrosion," Corrosion, vol. 72, no. 10, pp. 1300-1310, 2016.

6. Y. Chen, S. Chen, and Y. Lei, "Surface Structure and Anti-Corrosion Properties of Copper Treated by a Dopamine-Assisted 11-Mercaptoundecanoic Acid Film," Corrosion, vol. 68, pp. 747-753, 2012.

7. Z. Belarbi, T. N. Vu, F. Farelas, M. Singer and S. Nesic, "Thiols as volatile corrosion inhibitors for top of the line corrosion," Corrosion, vol. 73, no. 7, pp. 892-899, 2017.

8. Z. Belarbi, F. Farelas, D. Young, M. Singer, and S. Nesic, " Effect of different parameters on the inhibition efficacy of decanethiol," in CORROSION/2018, paper no. 10823, Houston, TX: NACE 2018.

9. J. M. Dominguez Olivo, B. Brown, and S. Nesic, "Modeling of corrosion mechanisms in the presence of quaternary ammonium chloride and imidazoline corrosion inhibitors," in CORROSION/2016, paper no. 7406, Houston, TX: NACE, 2016.

10. J.M. Dominguez Olivo, D. Young, B. Brown and S. Nesic, "Effect of corrosion inhibitor alkyl tail length on the electrochemical process underlying CO_2 corrosion of mild steel," in CORROSION/2018, paper no. 11537, Houston, TX: NACE.

11. D.M. Adams, L. Brus, C. E. D. Chidsey, S. Creager, C. Creutz,| C. R. Kagan, P. V. Kamat, M. Lieberman, S. Lindsay, R. A. Marcus, R. M. Metzger, M. E. M. Beyerle, J. R. Miller, M. D. NewtonD. R. Rolison, O. Sankey, K. S. Schanze, J. Yardley and X. Zhu, "Charge Transfer on the Nanoscale: Current Status," The Journal of Physical Chemistry B, vol. 107, pp. 6668–6697,2003.

12. M. Knag, K. Bilkova, E. Gulbrandsen, P. Carlsen, and J. Sjöblom, "Langmuir–Blodgett films of dococyltriethylammonium bromide and octadecanol on iron. Deposition and corrosion inhibitor performance in CO_2 containing brine," Corrosion Science, vol. 48, pp. 2592-2613, 2006.

13. F. Farelas, M. Galicia, B. Brown, S. Nesic and H. Castaneda, "Evolution of dissolution processes at the interface of carbon steel corroding in a CO_2 environment studied by EIS," Corrosion Science, vol. 52, pp. 509-517, 2010.

14. I. Epelboin and M. Keddam, "Faradic impedance: diffusion impedance and reaction impedance," Journal of Electrochemical Society, vol. 117, pp. 1052-1056, 190.

15. B. Hirschhorn, M. E. Orazem, B. Tribollet, V. Vivier, I. Frateur and M. Musiani, "Constant-phase-element behavior caused by resistivity distribution in films. I. Theory," Journal of Electrochemical Society, vol. 157, no. 12, pp. C452-C457, 2010.

16. P. Altoe, G. Pimenta, C.F. Moulin, S.L. Díaz and O.R. Mattos, "Evaluation of oilfield corrosion inhibitors in CO_2 containing media: a kinetic study", Electrochimica Acta, vol. 41, pp. 1165-1172,1996.

17. D.S. Carvalho, C.J.B. Joia and O.R. Mattos, "Corrosion rate of iron and iron-chromium alloys in CO_2 medium", Corrosion Science, vol. 47, pp. 2974-2986,2005.

18. T. Almeida, M.C.E. Bandeira, R.M. Moreira and "O.R. Mattos, New insights on the role of CO_2 in the mechanism of carbon steel corrosion", Corrosion Science, vol. 120, pp. 239-,2017.

19. K.L.J. Lee and S. Nesic, "The effect of trace amounts of H_2S on CO_2 corrosion investigated by using EIS technique", in CORROSION/2005, paper no. 360, Houston, TX: NACE.

20. G. J. Brug, A. G. V. D. Eeden, M. Sluyters-Rehbach and J. H. Sluyters, "The analysis of electrode impedances complicated by the presence of a constant phase element," Journal of Electroanalytical Chemistry, vol. 176, pp. 275-295, 1984.

21. D. Staicopolus, "The role of cementite in the acidic corrosion of steel," Journal of Electrochemical Society, vol. 110, no. 11, pp. 1121-1124, 1963.

22. K. Videm, J. Kvarekvaal, T. Pérez, and G. Fitzsimons, "Surface Effects on the electrochemistry of iron and carbon steels electrodes in aqueous CO_2 solution," in CORROSION/96, paper No.1, NACE,, Houston, TX, 1996.

23. S. Al-Hassan, B. Mishra, D. Olson, and M. Salama, "Effect of microstructure on corrosion of steels in aqueous solutions containing carbon dioxide," Corrosion, vol. 54, no. 6, pp. 480-491, 1998.

24. K. Marušić, H. O. Ćurković, and H. Takenouti, "Inhibiting effect of 4-methyl-1-p-tolylimidazole to the corrosion of bronze patinated in sulfate medium," Electrochemica Acta, vol. 56, pp. 7491-7502, 2011.

25. F. S. Damos, R. C. S. Luz, and L. T. Kubota, "Determination of Thickness, Dielectric Constant of Thiol Films, and Kinetics of Adsorption Using Surface Plasmon Resonance," *Langmuir*, vol. 21, pp. 602-609, 2005.

26. M. A. Rampi, O. J. A. Schueller and G. M. Whitesides, "Alkanethiol self-assembled monolayers as the dielectric of capacitors with nanoscale thickness," Applied Physics Letters, vol. 72, no.14, pp.1781-1783, 1998.

27. J. F. Scamehorn, R. S. Schechter, and W. H. Wade, "Adsorption of Surfactants on Mineral Oxide Surfaces from Aqueous Solutions .1. Isomerically Pure Anionic Surfactants," Journal of Colloid and Interface Science, vol. 85, pp. 463-478, 1982.

28. C. Pirlot, J. Delhalle, J. Pireaux, and Z. Mekhalif, "Surface modification of polycrystalline iron surfaces by n-dodecanethiol: an XPS investigation," Surface and Coatings Technology, vol. 138, pp. 166-172, 2001.

29. H. Zhang, C. Romero and S. Baldelli, "Preparation of Alkanethiol Monolayers on Mild Steel Surfaces Studied with Sum Frequency Generation and Electrochemistry," The Journal of Physical Chemistry B, vol. 109, pp. 15520-15530, 2005.